VOL. 20, NO. 2-2, 2021, 120-125
www.elektrika.utm.my
ISSN 0128-4428

ELEKTRIKA
Journal of Electrical Engineering

A Study of MEMS-Based Micro-Electro-Discharge Machining and Application to Micromanufacturing

Ningyuan Wang* and **Kenichi Takahata**

Department of Electrical and Computer Engineering, The University of British Columbia, 2332 Main Mall, Vancouver, BC V6T 1Z4, Canada.

*Corresponding author: Wangnyuan@hotmail.com

Abstract: MEMS-based micro-electro-discharge machining (M^3EDM) is a batch microfabrication technique that utilizes planar-electrode actuators fabricated directly on the work material. Electrostatically driving the electrode-actuator device, previously enabled with copper-based designs, using an applied EDM voltage enables micromachining of electrode patterns into any electrically conductive material. This paper presents an alternative device based on nickel with its higher thermomechanical resistance, aiming to achieve greater uniformity and stability of the process toward its application to micromanufacturing. The developed nickel-based device and its M^3EDM process is used to pattern cantilever-like MEMS contact switches as a preliminary application test, demonstrating the process with the intended effects. The outcome is analyzed to suggest a need for improvement, which is addressed through a modified approach to the M^3EDM fabrication of application devices showing a promising result. The study encourages further optimizations of the technology, which are evaluated and discussed as well.

Keywords: Micro-electro-discharge machining, micro-electro-mechanical systems, microfabrication, electrostatic actuators, micromanufacturing.

Article History: received 25 May 2021; accepted 12 June 2021; published 15 September 2021..

1. INTRODUCTION

Electro-discharge machining (EDM) is a thermomechanical machining process. Traditionally, EDM has been applied to machine hard metals and alloys into complex geometries in a dielectric fluid (EDM oil). The controlled generation of miniaturized pulses of spark discharge with combinational use of precision positioning systems enabled micro-scale EDM (µEDM), which has been used as means to create metal microstructures with high aspect ratios and good surface quality [1, 2]. This attractive method has enabled precision micromachining of nontraditional MEMS materials from hard alloys such as WC-Co [3] to soft materials such as carbon nanotube forests [4]. Micro-electro-mechanical systems (MEMS) fabricated using µEDM, e.g., shape-memory-alloy stents [5] and capacitive pressure sensors [6] have been reported in numerous papers as well. However, conventional µEDM, which employs scanning of a single cylindrical electrode to shape structures individually, is a serial process that suffers from low throughput [7]. The process also requires expensive numerical control (NC) systems for electrode positioning control [8]. Batch-mode µEDM was developed to address these fundamental issues of µEDM. This technique uses an array of high-aspect-ratio microstructures as the tool electrode to achieve a parallel machining process [9]. A developed batch-mode process was reported to offer >100· throughput compared to the serial µEDM process [10].

MEMS-based µEDM (M^3EDM) is a new concept for batch-mode µEDM that leverages MEMS actuators to enable the parallel process (Figure 1). This approach was proposed to achieve micromanufacturing of MEMS and other devices at low cost by scaling up the parallelism of µEDM while eliminating the need for NC systems from the µEDM process. The µEDM removal is achieved by fabricating MEMS actuators directly on a workpiece together with pre-patterned planar electrodes and electrostatically driving them to generate discharge pulses using a machining voltage applied. The geometries of the planar electrodes are designed for batch-mode, high-

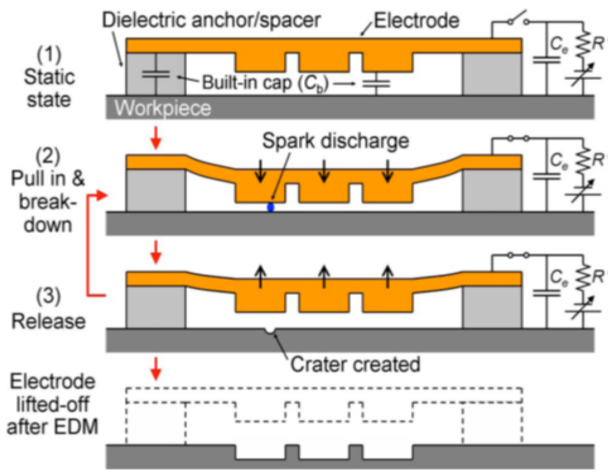

Figure 1. The machining principle of M^3EDM [12]. Copyright 2010, IEEE.

throughput pattern transfer to the workpiece. Promising results have been reported from previous efforts using copper-based devices [11, 12]. However, this device design was observed to exhibit certain deformation in the electrode structures leading to the non-uniformity in the process. The device's structural integrity can be degraded via different mechanisms. The wear of the electrodes is one of them. In any EDM process, its electrode is also thermomechanically attacked to be consumed [13]. The heat generated by the discharge may lower the structural precision due to a softening mechanism [14] based on the fact that the hardness of metals decreases below their melting points (250 °C or lower for copper) [15, 16]. Further, the instant expansion of the bubbles generated in a narrow (1-10 μm) space of the EDM fluid sandwiched between the suspended planar electrode and a fixed workpiece by each discharge heat applies pulsed shockwaves to the electrode [8], potentially causing metal fatigues in the structure [17].

To overcome these effects, metals other than copper could be adopted as more effective electrode-actuator material. A material with higher melting point is shown to have a higher wear resistance independent of the workpiece material [18]. The use of such material with higher hardness facilitates greater resistance to the thermal softening. The elastic modulus of the actuator material greatly affects the driving voltage. For example, using a stiffer material leads to the need for a higher voltage to make an electrode's displacement necessary to trigger discharge, which in turn causes poorer machining quality due to a resultant higher discharge energy used to remove the work material. Nickel is a potentially good candidate under these conditions. Given its higher melting/softening point and higher hardness than copper, the use of nickel could address the deformation problem. However, nickel is not a preferred electrode material for EDM due to low machining efficiency [19]. Combining the copper electrodes with the nickel device platform could yield higher performance than the case of a single-material design. The current work investigates this approach to the M^{3}EDM devices and processes. The fabrication of a preliminary application device using the developed processes is also investigated and discussed.

2. WORKING PRINCIPLE AND DESIGN

As shown in Figure 1Figure , the planar electrode is suspended on top of the workpiece. The two elements are electrically isolated by the dielectric anchors with a designed gap spacing. A resistor-capacitor (RC) pulse generation circuit [10] with a DC source of relatively high voltage (~100 V) is connected to them (step-1). Upon turning on the power, the capacitor is fully charged, whose voltage is applied between the electrode and the workpiece. This voltage generates an electrostatic force to pull the suspended electrode down toward the workpiece. The voltage is made higher than the pull-in voltage [20], so that the electrode moves down to almost collapse on the workpiece. Before physically touching down, however, a spark is ignited (step-2) while the capacitor discharges to create a current pulse, instantly lowering the voltage at the gap thereby dissipating the force acting on the electrode (step-3). However, since electrode's mechanical response in the EDM fluid is much slower than the charging cycle of the RC circuit to recover the force, the electrode stays at the lowered position stably while steps-2 and -3 are repeated, continuing to generate discharge pulses and etch the workpiece. The electrode follows the workpiece surface being etched while maintaining the discharging gap, transferring its pattern to the workpiece.

There are two types of the device designs, namely single-layer and double-layer designs (refer to the last step in Figure 3(a) and 3(b), respectively) [11, 12]. In the former case, a copper foil seamlessly forms the planar electrode and actuator structure, which was demonstrated to cut micro pillars on a stainless-steel substrate [11]. The double-layer device accommodates electroplated patterns underneath the actuator platform all made of copper, which was used for patterning of cavity arrays [12]. The current work for the nickel-based devices follows these two forms, with a crab-leg spring design (Figure 2) to exploit its relatively large electrode/machining area with

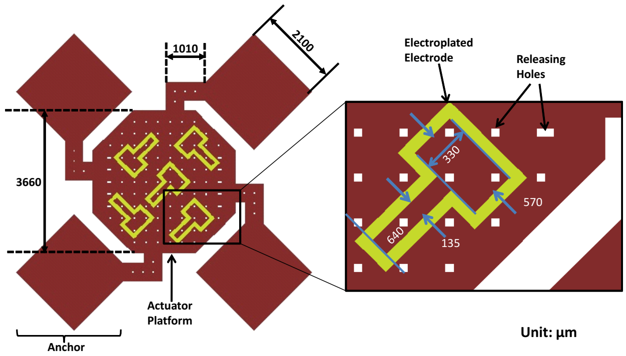

Figure 2. An example of the M^{3}EDM device designed for fabrication of test MEMS switch devices.

more uniform actuation displacements compared with other options (e.g., cantilevers).

As a test application of the developed M^{3}EDM, the double-layer device is designed to micromachine a cantilever-like MEMS contact switch by cutting into a metal foil fixed on the polymer-coated metal substrate. The maximum cutting depth is an important factor to complete this type of process [12]. It represents the threshold depth where the upward spring restoring force, F_{spring}, exceeds the downward electrostatic force, $F_{electro}$, both acting on the actuator platform. The above threshold condition can be expressed as [12]:

$$F_{spring} = K(x_{max} + d_0 - g) \equiv F_{electro} \cong \frac{\varepsilon A}{2g^2} V^2 \quad (1)$$

where K is the overall spring constant of the device, x_{max} is the projected maximum machining depth, g is the discharging gap, d_o is the initial electrode-workpiece gap, A is the equivalent area of the electrode, and V is the voltage applied. The thickness of the metal foil to be cut is set to be 10 μm in the particular process. The thickness of the polymer (photoresist) sacrificial layer sandwiched between the above foil and the substrate is selected to be 10 μm as well in this design.

3. M^{3}EDM DEVICE FABRICATION

The nickel-based devices are fabricated on a 3" stainless-steel wafer serving as the substrate to be μEDMed. The fabrication approach is similar to the one demonstrated for the copper devices [12]. The single-layer devices are fabricated by stacking layers on the substrate (Figure 3(a)), whereas the electrode and substrate structures are prepared separately and bonded together to fabricate the double-layer devices (Figure 3(b)). The substrate structure is prepared by spin-coating an adhesion promoter (MCC Primer 80/20, MicroChem, MA, USA) and then a sacrificial photoresist layer (SPR-220-7, Rohm Haas, PA, USA) with a thickness of 30-35μm for the single-layer or 10-15 μm for the double-layer process, followed by soft baking at 90 °C. Both the single- or double-layer processes use 15-μm-thick nickel foil.

The double-layer electrode structure is fabricated as follows. First, through-hole alignment markers are pre-patterned on the nickel foil using photo-defined wet etching (Nickel Etchant Type I, Transene, MA, USA). The foil is then uniformly fixed onto a temporary glass substrate using tape. Next, a thick (35-40 μm) SPR-220-7 is spun on the foil and soft baked for 30 minutes. The photoresist is left in air for at least 12 hours to restore the moisture level. The photoresist is then patterned using a mask aligner and developed to form an electroplating mold (with the patterns of a target device), followed by electroplating to form 30-μm-thick copper electrodes on the nickel foil. After this, the electroplated foil is removed from its temporary substrate and bonded onto the substrate structure using a spin-coated 1-μm-thick photoresist (S1813, Rohm Haas, MA, USA) as an adhesive layer via soft baking for 5 minutes. Individual M^{3}EDM devices are shaped using the photo-defined wet etching (same as the single-layer process). Finally, their electrodes are released using acetone to complete the fabrication (Figure 4).

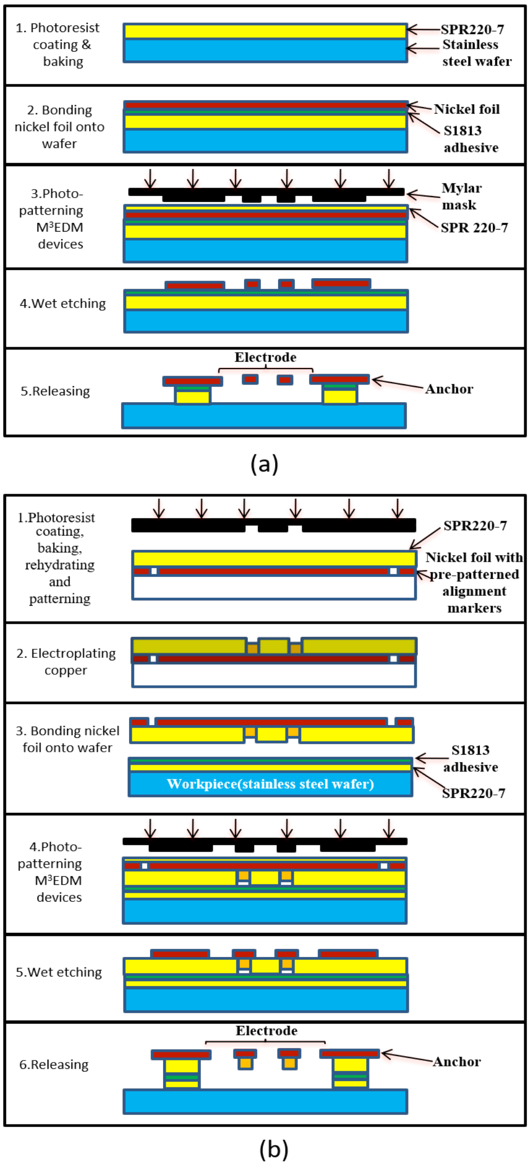

Figure 3. Fabrication process for nickel-based devices: (a) Single-layer device, and (b) double-layer device.

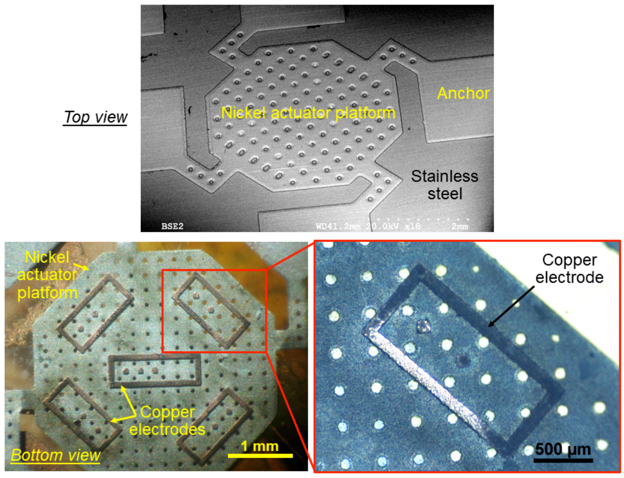

Figure 4. An example of fabricated double-layer nickel device with copper electrodes (bottom image taken by peeling the device from the substrate) after μEDM use.

4. EXPERIMENTAL RESULTS AND DISCUSSION

The fabricated devices were tested using the experiment set-up shown in Figure 5. The wafer sample was fixed onto the sample holder (with a thick glass plate as shown for insulation purpose), placed in an ultrasonic bath of EDM fluid (EDM 185, Commonwealth Oil Co, ON, Canada). The ultrasonic function was used to effectively remove machining byproducts from the sample. The RC circuit was configured with a 20-kΩ resistor and a 100-pF capacitor. This circuit was coupled with a short-circuit limiter that automatically detected shorting between the electrode and the substrate during μEDM and prevented harmful thermal impacts caused by it. The discharge pulse currents were monitored during the process in real

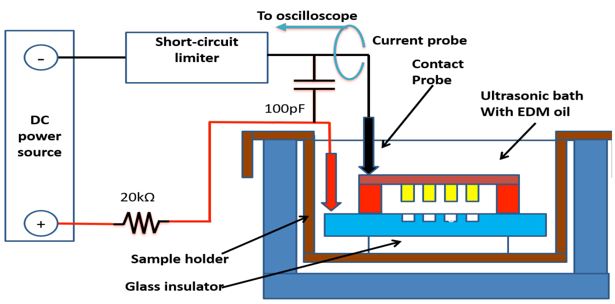

Figure 5. Experimental set-up of M^{3}EDM tests.

time using an inductive current probe (CT-2, Tektronix, TX, USA) coupled with the RC circuit.

The single-layer devices were first tested. The deformation of the electrode in the discharging area was clearly suppressed compared with the previous copper device case. However, as expected, the machining process was not stable to sustain even by applying higher voltages (e.g., 150 V). More effective processing was achieved using the double-layer devices with the electroplated copper electrodes, showing a stable and sustainable machining process (observed for a duration of up to 30 minutes). The voltage necessary to trigger discharges (~100 V) was lower than an estimated pull-in voltage (~150 V). Mechanical effects led by the presence of etch holes in the crab legs as well as excessive removal of nickel in its isotropic wet etching can be the potential reasons (in a way to lower the apparent spring constant, *K*) behind this outcome.

The M^{3}EDM process studied for the contact switch formation is illustrated in Figure 6. μEDM is inherently capable of machining any electrically conductive material to provide broad application opportunities in MEMS and other areas. For experimental verification purpose, the current study used copper foil (10-μm thickness) as the layer to machine the cantilever patterns. These copper patterns can then be used to complete the suspended switch structures on a metal wafer via sacrificial etching (this final step after M^{3}EDM patterning is not included in the current test). The substrate and electrode structures were prepared through the processes similar to those used for the substrate structure of the single-layer device (Figure 3(a), except for using the copper (instead of nickel) foil and the 10-μm-thick sacrificial layer) (step-1), and the electrode structure of the double-layer device (Figure 3(b)), respectively. The double-layer devices were fabricated by bonding the electrode structure onto the substrate one, followed by photo-defined shaping of the M^{3}EDM devices and releasing the electrodes (step-2). The electrodes were then driven to cut into the copper foil to shape the switch patterns by μEDM. The M^{3}EDM devices were stripped away once the switch patterns were fully separated from the foil (step-3). In the last step, the cantilever structures are released by sacrificial etching while the remaining foil is stripped off (step-4).

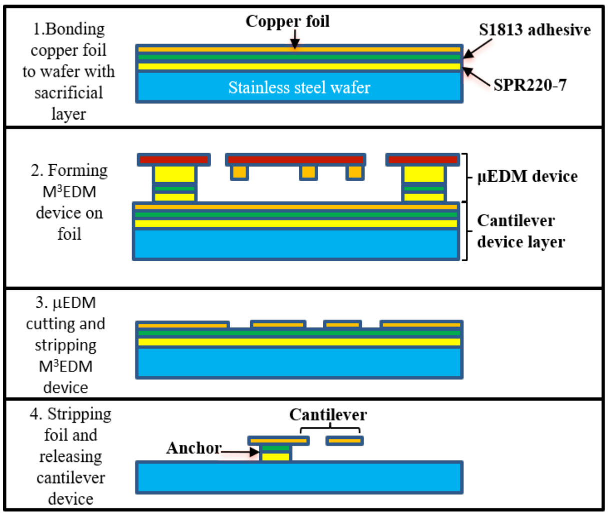

Figure 6. M^{3}EDM process for the test fabrication of the contact switch device.

The nickel-based M^{3}EDM devices were successfully fabricated on the copper foil of the substrate structure. Applying a voltage of 100-150 V, electrode actuation and μEDMing was observed; however, complete cutting of the foil did not reach even after an extended machining time. It was found that the electrode patterns were fully transferred onto the foil but with no penetration (Figure 7(a)). Careful observation of the machined regions revealed that the patterns were not only transferred to the foil but also to the photoresist layer (Figures 7(c) and 7(d)). The patterns were clearly observed on the backside of the foil as well (Figure 7(b)). The glass transition temperature (T_g) of SPR220-7 (patterned and soft baked) was reported to be below 150 °C [21]. Given the fact that temperature of each discharge pulse can reach several 1000's °C [22] while the machining region is repeatedly exposed to this level of temperature at a high frequency (in the 100 kHz range for the circuit used), the amount of discharge-induced heat transferred from the copper foil being machined to the SPR220-7 layer underneath was potentially sufficient to raise its temperature over the T_g and consequently melt the layer. This in turn can lead to certain deformation of the copper foil as well, which might have prevented it from being completely cut and penetrated by the planar electrodes.

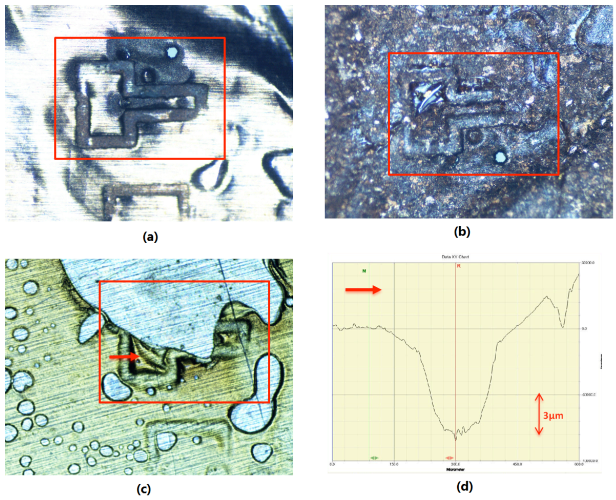

Figure 7. A sample patterning result showing the same region (indicated with a red box) of different surfaces/layers after the process: (a) Front side of the copper foil, (b) backside of the foil, (c) SPR220-7 photoresist layer under the foil (part of the layer damaged during stripping the foil), and (d) a stylus-measured profile along the arrow shown in (c) indicating a concave profile of the pattern with a depth of ~6 μm seen on the photoresist layer.

One straightforward solution to the above problem is to use a dielectric material with high thermal stability as the sacrificial layer beneath the copper foil. Certain polymers such as polyimide [23] and SU-8 (epoxy-based photoresist) [24] as well as spin-on glass (SOG) [25] offer high thermal stability; however, sacrificial etching of these polymers is challenging once cured, and the available thickness of SOG is rather limited. Minimizing the impact of photoresist layer deformation on the patterning process is another potential solution to the problem. A modified process was investigated for this purpose. This process adds a pattern transfer step to eliminate the thick photoresist underneath the foil to be µEDMed (The foil was uniformly bonded onto a temporary thin (100 µm) glass substrate with a 1-µm-thick S1813 spin-coated as the adhesive layer (step-1). The double-layer devices were then fabricated on this glass substrate, performing µEDM to create the switch patterns (step-2) and then striping the used M^3EDM devices off (step-3). To complete the switch devices, the patterned copper structures are bonded on and transferred to the wafer coated with the thick SPR220-7 and adhesive layer, followed by fully dissolving the glass substrate in a hydrofluoric-acid solution (step-4) and sacrificial etching in acetone to release the switch structures (step-5).

Owing to the 10-15· smaller thickness (1 µm) of the photoresist under the foil, the new process was successful in suppressing the thermal deformation problem. In fact, the machining results showed a clear improvement. As displayed in , the copper foil was penetrated for 60-70 % of the electrode pattern, unlike the case of the original process (Figure 6) that provided 0% penetration as discussed earlier. This outcome however indicates that the process still needs further improvement for the full-pattern penetration. The incomplete penetration could be due to different potential causes, including the thickness non-uniformity in the spin-coated sacrificial (mainly SPR 220-7) layer, thermal softening/deformation of this layer led by the bonding step, and height non-uniformity in the electroplated copper electrodes. Addressing the first and second factors will require optimization of the photoresist coating and baking steps while minimizing its thickness

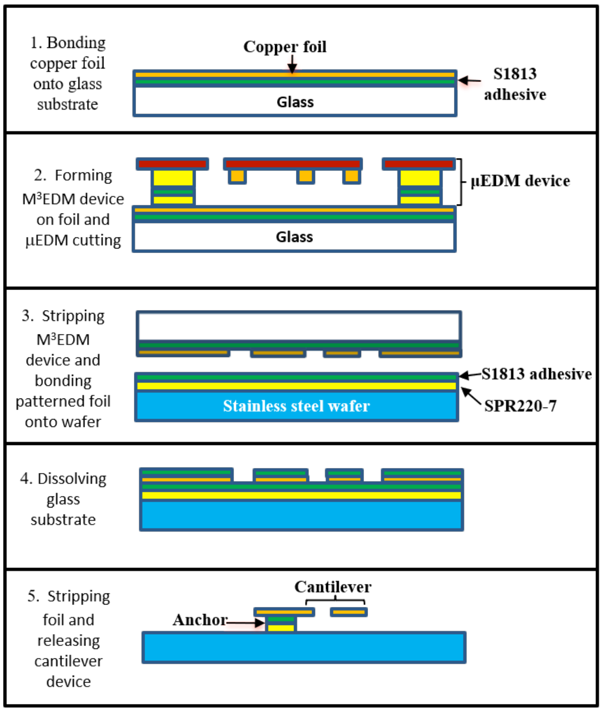

Figure 8. Modified M^3EDM process for the test fabrication of the contact switch device.

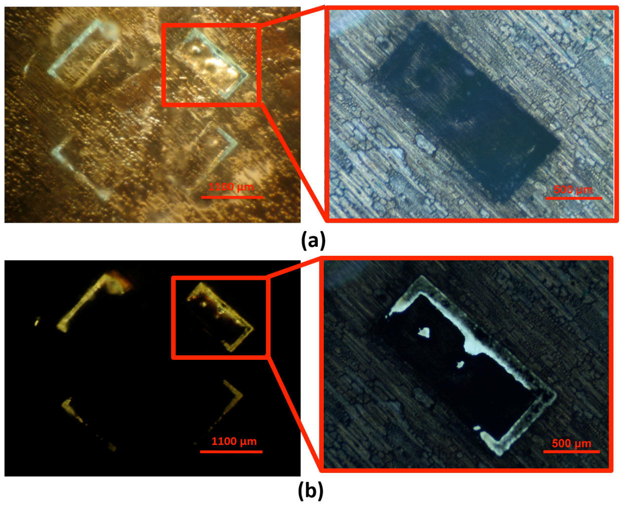

Figure 9. A sample patterning result obtained with the modified M^3EDM process (using the electrodes with a rectangle pattern shown in Figure 4): (a) Backside of the machined area with front illumination (left) and a close-up view (right), and (b) backside of the same machined area with background illumination (left) and a close-up view (right).

needed for the sacrificial process or the anchor height of the M^3EDM device. A higher uniformity of the electroplated structures can be approached by adding a lapping/polishing step after electroplating. Another merit of the modified process (Figure 8) is the availability of visual observation of the machining progress directly from the backside of the glass substrate (without needing to remove the M^3EDM devices). This unique feature can be leveraged for further optimization of the M^3EDM device structures and patterning process.

6. CONCLUSIONS

This work has investigated M^3EDM with improved device designs and fabrication processes. Nickel-based electrode-actuator devices were studied and developed to experimentally demonstrate more stable µEDM with the double-layer design compared with those based on copper. The developed process was applied for batch fabrication of a test MEMS device via parallel patterning of metal foil using the developed M^3EDM. The sacrificial-layer softening issue, presumably led by discharge-induced heat, was addressed by developing a modified M^3EDM method. The results revealed an improved outcome and the effectiveness of the alternative method while indicating the need for additional improvement in patterning uniformity. Based on the results obtained, future work encompasses further optimization of the device design and process control for high-throughput, high-uniformity M^3EDM toward its application to micromanufacturing.

ACKNOWLEDGMENTS

This work was supported by the Natural Sciences and Engineering Research Council of Canada and CMC Microsystems. K. Takahata was supported by the Canada Research Chairs program.

REFERENCES

[1] M. D. T. Pham, S. S. Dimov, S. Bigot, A. Ivanov, and K. Popov, "Micro-EDM--recent developments and research issues," *Journal of Materials Processing Technology*, vol. 149, no. 1, Jun. 2004, pp. 50-57.

[2] M. J. Madou, "Fundamentals of microfabrication: the science of miniaturization". *CRC Press*, 2002, pp. 398-401.

[3] K. Takahata, N. Shibaike, and H. Guckel, "High-aspect-ratio WC-Co microstructure produced by the combination of LIGA and micro-EDM," *Microsystem Technologies*, vol. 6, no. 5, 2000, pp. 175-178.

[4] W. Khalid, M.A. Mohamed Sultan, M. Dahmaredeh, Y.Choi, P. Yaghoobi, A. Nojeh and K. Takahata, "High-aspect-ratio, free-form patterning of carbon nanotube forests using micro-electro-discharge machining," *Diamond and Related Materials*, vol. 19, no. 11, Nov. 2010, pp. 1405-1410.

[5] K. Takahata, Y. Gianchandani, and K. Wise, "Micromachined Antenna Stents and Cuffs for Monitoring Intraluminal Pressure and Flow," *Microelectromechanical Systems*, Journal of, vol. 15, no. 5, 2006, pp. 1289-1298.

[6] K. Takahata and Y. B. Gianchandani, "A Micromachined Capacitive Pressure Sensor Using a Cavity-Less Structure with Bulk-Metal/Elastomer Layers and Its Wireless Telemetry Application," *Sensors*, vol. 8, no. 4, 2008, pp. 2317-2330.

[7] K. Takahata, S. Aoki, and T. Sato, "Fine surface finishing method for 3-dimensional micro structures", *JEICE Trans. Electronics*, vol. E80-C, no. 2, 1997, pp. 291-296.

[8] M. Kunieda, B. Lauwers, K. Rajurkar, and B. Schumacher, "Advancing EDM through Fundamental Insight into the Process," CIRP Annals - *Manufacturing Technology*, vol. 54, no. 2, 2005, pp. 64-87

[9] H. H. Langen, T. Masuzawa, and M. Fujino, "Modular method for microparts machining and assembly with self-alignment", *Annals of the CIRP*, vol. 44, 1995, pp. 173-176.

[10] K. Takahata and Y. B. Gianchandani, "Batch mode micro-electro-dischargemachining", *IEEE/ASME Journal of Microelectromechanical Systems*, vol. 11, 2002, pp. 102-110.

[11] C. R. A. Chaitanya and K. Takahata, "M^3EDM MEMS-enabled micro electro discharge machining" *Journal of Micromechanics and Microengineering*, vol. 18, no. 10, 2008, p. 105009 (7pp).

[12] C. Chaitanya, N. Wang, and K. Takahata, "MEMS-Based micro-electro-discharge machining (M^3EDM) by electrostatics actuation of machining electrodes on the workpiece", *IEEE/ASME Journal of Microelectromechanical Systems*, vol. 19, no. 3, 2010, pp. 690-699.

[13] S. H. Yeo, W. Kurnia, and P. C. Tan, "Electro-thermal modelling of anode and cathode in micro-EDM," *Journal of Physics D: Applied Physics,* vol. 40, no. 8, 2007, pp. 2513-2521.

[14] S. H. Yeo, E. Aligiri, P. C. Tan, and H. Zarepour, "A New Pulse Discriminating System for Micro-EDM," *Materials and Manufacturing Processes*, vol. 24, no. 12, 2009, pp. 1297-1305.

[15] A. Broue et al., "Validation of bending tests by nanoindentation for micro-contact analysis of MEMS switches," *Journal of Micromechanics and Microengineering*, vol. 20, no. 8, 2010, p. 085025(8pp).

[16] A. Senouci, H. Zaidi, J. Frene, A. Bouchoucha, and D. Paulmier, "Damage of surfaces in sliding electrical contact copper/steel," *Applied Surface Science*, vol. 144, Apr. 1999, pp. 287-291.

[17] C. Dai, X. Zhu, and G. Zhang, "Tensile and Fatigue Properties of Free-Standing Cu Foils," *Journal of materials science & technology*, vol. 25, no. 06, 2009, pp. 721-726.

[18] Y. Tsai and T. Masuzawa, "An index to evaluate the wear resistance of the electrode in micro-EDM," *Journal of Materials Processing Technology,* vol. 149, no. 1, Jun. 2004, pp. 304-309

[19] N. Tantra, F. Leao, and I. Pashby, "Evaluating theoretical equations to predict wear in electro-discharge machining," in *Proceedings of the First International Conference and Seventh AUN/SEED-Net Fieldwise Seminar on Manufacturing and Material Processing,* 2006, pp. 151-155.

[20] S. Pamidighantam, R. Puers, K. Baert and H. A. C. Tilmans, "Pull-in voltage analysis of electrostatically actuated beam structures with fixed -fixed and fixed-free end conditions", *Journal of Micromechanics and Microengineering*, vol 12, pp 458-464

[21] E. Roy, B. Voisin, J. Gravel, R. Peytavi, D. Boudreau, and T. Veres, "Microlens array fabrication by enhanced thermal reflow process: Towards efficient collection of fluorescence light from microarrays," *Microelectronic Engineering*, vol. 86, no. 11, Nov. 2009, pp. 2255-2261.

[22] S. Dhanik and S. S. Joshi, "Modeling of a single resistance capacitance pulse discharge in micro-electro discharge machining", *Journal of Manufacturing Science and Engineering*, Nov. 2005, vol. 127, Iss 4, pp. 759-767.

[23] D. N. Khanna and W. H. Mueller, "New high temperature stable positive photoresists based on hydroxy polyimides and polyamides containing the hexafluoroisopropylidene (6-f) linking group," *Polymer Engineering and Science*, vol. 29, no. 14, 1989, pp. 954-959.

[24] A. D. Campo and C. Greiner, "SU-8: a photoresist for high-aspect-ratio and 3D submicron lithography," *Journal of Micromechanics and Microengineering*, vol. 17, no. 6, 2007, pp. R81-R95.

[25] A. A. Hamzah, B. Y. Majlis, and I. Ahmad, "Formation of thick spin-on glass (SOG) sacrificial layer for capacitive accelerometer encapsulation," in *Device and Process Technologies for Microelectronics, MEMS, and Photonics IV*, vol. 6037, 2005, pp. 227-237.